Pergamon

Cement and Concrete Research 31 (2001) 925–931

CEMENT AND CONCRETE RESEARCH

Microstructural changes caused by carbonation of cement mortar

Björn Johannesson*, Peter Utgenannt

Division of Building Materials, Lund Institute of Technology, P.O. Box 118, SE-221 00 Lund, Sweden

Received 29 November 2000; accepted 28 February 2001

Abstract

The change of specific surface area and pore size distribution due to carbonation of an ordinary Portland cement mortar is investigated. The adsorption of water vapor on noncarbonated and well-carbonated cement mortar is measured in order to evaluate the difference in specific surface area for the two samples using the BET theory. From the measured desorption the pore size distribution is calculated using the Kelvin formula. A sorption balance is used to measure the sorption characteristics for the two studied sample qualities. In this method dry and saturated air are mixed in desired proportion in a closed system. One of the benefits of the method is that the samples not are exposed to carbon dioxide during testing, i.e., undesired effects caused by carbonation on the sorption can be eliminated. The specific surface area for a noncarbonated sample was calculated, using the measured adsorption data, to be 8% higher than for the well-carbonated sample. The difference in pore size distributions was more marked than the difference in specific surface area for the two samples. The well-carbonated mortar had about twice as much volume attributed to small pores as the noncarbonated cement mortar. © 2001 Elsevier Science Ltd. All rights reserved.

Keywords: Cement mortar; Carbonation; Sorption; Pore size; Distribution; BET equation

1. Introduction

Carbonation and its microstructural effects on cement paste are investigated by measuring adsorption and desorption on noncarbonated and well-carbonated mortars. The BET method is used to calculate the specific surface area from the measured adsorption isotherm. The standard one-layer BET equation was used. The pore size distribution was estimated by the Kelvin and Laplace equations together with the use of measured data on desorption. The adsorption and desorption were measured using a dynamic vapor sorption (DVS) instrument. This instrument constitutes of a symmetric balance with a reference and a sample pan placed in a closed system. The relative humidity in the closed system is controlled by flow regulators by mixing dry and saturated gas. The dry gas used is nitrogen and the saturated condition is obtained by letting dry nitrogen flow across a liquid bath. Owing to the closed system and the gas used in the experiments the carbonation of the cement mortar sample during measurements was kept to a minimum.

By using the BET equation and the Kelvin and Laplace relations together with measured data on adsorption and desorption it is concluded that the specific surface area for the carbonated and noncarbonated sample differed very little. The pore size distribution evaluated from the desorption test was, however, different for the two tested samples, in which the well-carbonated samples had a significantly larger part of the porosity attributed to cylinders with small pore radii.

2. Experimental procedure

Carbonated and noncarbonated cement mortar was investigated with respect to adsorption and desorption behavior. The composition of ordinary Portland cement mortar tested is shown in Table 1. The mortar was cast in small cylindrical plastic molds that were immediately sealed to prevent early carbonation. After 14 days the mortar cylinders were cut into 3-mm thick discs. Half the discs were placed in a climate camber [1] with a relative humidity of 65% and a temperature of 20°C and with an increased carbon dioxide content of maximum 1 vol.% CO_2. The remaining discs were placed in an identical climate chamber with a relative

---

* Corresponding author. Tel.: +46-46-222-4052; fax: +46-46-222-4427.

E-mail address: bjorn.johannesson@byggtek.lth.se (B. Johannesson).

PII: S0008-8846(01)00498-7

Table 1
Mix proportions of the tested OPC mortar

	Mass density (kg/m^3)	Actual weight (kg)
Cement (OPC)	545	0.774
Aggregate 0–0.125 mm	422	0.600
Aggregate 0.125–0.250 mm	422	0.600
Aggregate 0.250–0.500 mm	422	0.600
Water	300	0.426

Water to binder ratio 0.55. OPC = ordinary Portland cement (Degerhamn standard [2] is a low alkali, sulfur-resistant cement).

humidity of 65% and a temperature of 20°C but with an environment free from carbon dioxide. After about 4 months of conditioning in the climate chambers the carbonation depth of the mortar discs was measured using a phenolphthalein indicator. The discs stored in the environment with increased carbon dioxide did not show any color change using the indicator, thus the mortar was fully carbonated. The discs stored in the environment free from carbon dioxide were shown, using the same procedure, not to be carbonated. Some discs were then crushed to powder using a mortar and pestle. Mortar powder from specimens conditioned in the two different climates was then tested for water adsorption and desorption using a DVS-1000 sorption balance (see Fig. 1).

The sorption balance used measures the weight of small samples by a sensitive microbalance while the sample is exposed to a relative humidity program. The symmetrically arranged balance measures changes in mass lower than 1 part in 10 million. The symmetric arrangement of the balance is used in order to avoid effects of sorption on the sample holder, i.e., the sorption on the sample holder and the reference holder in use cancel each other out. The instrument is housed in an incubator in which the temperature can be controlled. The closed system placed in the incubator contains the sample which is subjected to a relative humidity, obtained by mixing dry and saturated air. The desired relative humidity is obtained by flow regulators with high precision. Even though a certain relative humidity can be obtained by mixing dry and saturated air, using flow regulators, humidity probes are situated just below the sample and the reference holder to give independent verification of system performance.

An equilibrium adsorption isotherm can be obtained by letting the system gradually increase the relative humidity in the environment surrounding the predried sample in steps. The criterion for proceeding to a higher relative humidity is, typically, a prescribed value of the rate of mass change related to the dry mass of sample.

3. Carbonation of cement-based materials

Carbonation of Portland cement-based materials, i.e., the chemical reaction of calcium hydroxide and calcium silicate hydrate with carbon dioxide resulting in the formation of calcium carbonate and water, is one of the processes which takes place in the pores of concrete, and which may affect the service life. There are two main important consequences of carbonation: (i) the drop of pH, i.e., the drop in hydroxide concentration in the pore solution, which destroys the passive condition of embedded reinforcement bars, and (ii) the change of the effective permeability due to volume changes and microcracking caused by the chemical reactions. The permeability change can be an increase, as in concrete containing blast furnace slag or fly ash, or a decrease as in OPC-concrete, [3]. Measurements on carbonation of different kinds of concretes may, for example, be found in Ref. [4].

The final result of the several steps through which the calcium carbonate is formed may simply be described by the following reaction which is assumed to be irreversible.

$$\mathrm{CO_2(aq) + Ca^{2+}(aq) + 2OH^-(aq) \rightarrow CaCO_3(s) + H_2O}. \tag{1}$$

The dissolution of carbon dioxide in its gaseous phase is simply described as [Eq. (2)]

$$\mathrm{CO_2(g) \rightleftharpoons CO_2(aq)} \tag{2}$$

and the dissolution of calcium hydroxide as

$$\mathrm{Ca(OH)_2(s)^* \rightarrow Ca^{2+}(aq) + 2OH^-(aq)} \tag{3}$$

where the symbol (s)* is introduced to stress that the $Ca(OH)_2$ is arranged in a crystalline structure which is assumed to be intimately intergrown with the C-S-H, which is the more or less amorphous calcium silicate hydrate formed during hydration of C_3S and C_2S. The formed C-S-H also has a variable stoichiometry that makes the kinetics of the dissolution reaction (3) difficult to constitute, as the process most likely becomes diffusion-controlled at the microscopic level. The amount $Ca(OH)_2(s)^*$ is about 30 wt.% of the fully hydrated OPC. In blended cements like fly ash cement or slag cement the amount of $Ca(OH)_2$ is considerably lower. It should be observed that also C-S-H itself becomes carbonated. It is assumed

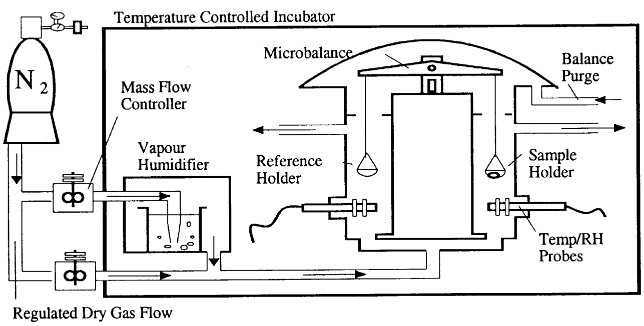

Fig. 1. Schematic sketch of the DVS instrument (DVS-1000). Dry and saturated air is mixed in desired proportions using flow regulators. The sample is placed on a symmetric microbalance to eliminate effects caused by sorption on holders.

that this reaction takes place in a similar way as carbonation of $Ca(OH)_2$. That is, C-S-H can be described as C-S-H = $3CaO \cdot SiO_2 \cdot 3H_2O = 3Ca(OH)_2 + SiO_2$. The carbonation of C-S-H probably occurs at a somewhat slower rate than the carbonation of 'pure' $Ca(OH)_2$. The solubility properties of the C-S-H may be studied in, for example, Ref. [5].

Actually, the dissolved CO_2 will form carbonic acid H_2CO_3(aq) together with water. H_2CO_3 will further be dissolved into $2H^+$ and CO_3^{2-} ions. Hence, reaction (1) can also be expressed as

$$Ca^{2+}(aq) + CO_3^{2-}(aq) \rightarrow CaCO_3(s). \tag{4}$$

The calcium carbonate formed has a very low solubility and will therefore contribute to a clogging of the pore system. However, the volume expansion involved in reaction (1) or (4) will cause microcracks in the carbonated zone. Therefore, it is difficult to predict the change of transport properties for gases, such as CO_2(g) and O_2(g), due to carbonation. The compressive and tensile strength of OPC are markedly increased due to carbonation [3]. This effect does not, however, give any explicit information about the changes of the transport properties.

As the formation of calcium carbonate requires that carbon dioxide diffuses from the atmosphere into the pores of the concrete and that calcium dioxide needs liquid water to form carbonic acid H_2CO_3(aq), Eqs. (1) and (4), the carbonation will be very largely ruled out if the pore system is filled with water, which will hinder the diffusion of carbon dioxide in its gaseous phase, or if the pore system is completely dry. The situation where pores are only partly filled with water is, however, a normal condition of concrete surfaces, making both diffusion of carbon dioxide in its gaseous phase and formation of carbonic acid possible.

The process of the decrease of pH due to carbonation in the pore solution is dependent on the relation between the rate of dissolution of the solid calcium hydroxide in Eq. (3) and the rate of consumption of OH^- in the carbonation process (1). However, when the solid calcium hydroxide at and near the pore walls is consumed, the dissolution process becomes more and more 'diffusion-controlled', and as a result the rate of dissolution of calcium hydroxide will gradually become slower. Therefore, a high concentration of hydroxide ions in the pore solution cannot be maintained when carbonation takes place.

The depth of carbonation is often determined with a phenolphthalein indicator, measuring the depth to the color change. Such tests only reveal the level where the pH value falls below about 9, and it is concluded that pore expression measurements in terms of hydroxide ion concentration in the pore solution are a better method that make it possible to measure the total pH profile. The decrease of hydroxide ion content is an indirect method to measure carbonation. SEM by backscatter electron imaging, however, makes it possible to study the $CaCO_3$ that forms. Such measurements show that a dense rim consisting largely of $CaCO_3$ is formed at the surface. Within this zone, CH is largely absent and C-S-H, including that formed in situ from the alite or belite, is decalcified in varying degrees. The carbonated surface layers are about 50–100 μm thick [3].

4. Evaluation of the specific surface area

From the measured adsorption isotherm the specific surface area can be calculated using the BET equation. The BET equation gives a relation between the volume content of adsorbate and the relative humidity during adsorption on material surfaces. The equation includes two constants, one of them related to the specific surface area and the other related to the energy required to place molecules on the bare material surface. The BET equation in use is

$$v = \frac{v_m c x}{(1-x)(1-x+cx)} \tag{5}$$

where v_m and c are the constants related to specific surface area and the heat of condensation of first layer adsorbate, respectively. The property v denotes the total volume of adsorbate at a certain relative humidity, denoted x. The BET equation is established by assuming that the condensation rates and evaporation rates from different discrete layers are related to the actual area occupied by different layers and to the pressure and temperature above the adsorbate. An equilibrium state is defined, for each discrete layer formed, in which an equal number of molecules are condensed and evaporated. The Ahrenius factor is involved in describing the rate of the evaporation/condensation phenomenon. That is, the effect of the temperature on the reaction rates is considered.

When it comes to matching the experimentally obtained function $v(x)$ with the BET equation, it is convenient to rewrite Eq. (5) as

$$\frac{x}{v(1-x)} = \frac{1}{v_m c} + \frac{(c-1)}{v_m c} x. \tag{6}$$

By plotting $x/(v(1-x))$ against x the result should be a straight line according to the BET equation. The slope is equal to $(c-1)/(v_m c)$ and the intercept is $1/(v_m c)$. From the slope and intercept the material constants c and v_m can be calculated.

The property v_m denotes the volume of gas corresponding to a complete monolayer covering the material surface. Therefore, the specific surface area can be predicted by assuming that a certain area is occupied by each adsorbed molecule on the adsorbate. Here it will be assumed that v_m is related to the specific surface area S as: $S = kv_m$, where $k = 3.54 \times 10^3$. The value of k is obtained by considering the mole weight and density of the adsorbate and by assuming that each water molecule, as studied in this case, occupies 10.6 $\AA^2$ on the adsorbent surface, a value based on the hypothesis that the water molecules are arranged in a close-packed pattern.

5. Estimation of pore size distribution

The pore size distribution can be estimated by using the measured desorption isotherm together with the Kelvin formula and the Laplace equation. In equilibrium defined by isothermal conditions and when no net mass exchange between vapor and adsorbed or capillary condensed water takes place, the relation between the chemical potential in the vapor and the adsorbed or capillary condensed water is given as

$$\frac{\partial\mu_v}{\partial\rho_v} = -\frac{\partial\mu_a}{\partial\rho_a} \tag{7}$$

where the chemical potential for the vapor μ_v and for the adsorbate μ_a are allowed to be functions of the temperature θ and mass density of vapor ρ_v and of adsorbate ρ_a only, i.e., $\mu_v = \mu_v(\theta, \rho_v)$ and $\mu_a = \mu_a(\theta, \rho_a)$. This assumption is referred to as the simple fluid assumption since μ_v is not allowed to depend on ρ_a and vice versa. Relation (7) is obtained by considering the second axiom of thermodynamics together with the physical balance laws for the special constitutive relations $\mu_v = \mu_v(\theta, \rho_v)$ and $\mu_a = \mu_a(\theta, \rho_a)$. Another relation which can be established by the same method for this case is a relation between the chemical potential of the adsorbate μ_a and the pressure in adsorbate p_a during isothermal conditions, given as

$$\rho_a\frac{\partial\mu_a}{\partial\rho_a} = \frac{\partial p_a}{\partial\rho_a}. \tag{8}$$

Assume, further, that the explicit constitutive relation for the chemical potential for the vapor is given as

$$\mu_v(\theta,\rho_v) = C_v\theta(1-\ln\theta) + \frac{R}{M_v}\theta\ln\rho_v. \tag{9}$$

By combining Eqs. (7)–(9) one obtains

$$\frac{\partial p_a}{\partial\rho_a} = -\frac{\rho_a R\theta}{M_v\rho_v} \tag{10}$$

which expresses the relation between the pressure in the vapor and the adsorbate. The integrated version of Eq. (10), with the opposite sign (i.e., $p_a = -p_{cap}$), can be interpreted as the so-called capillary pressure, i.e.

$$p_{cap} = \int_{\rho_v}^{\rho_{vs}} \frac{\rho_a R\theta}{M_v\rho_v} = -\frac{\rho_a R\theta}{M_v}\ln\left(\frac{\rho_v}{\rho_{vs}}\right) = -\frac{\rho_a R\theta}{M_v}\ln(x) \tag{11}$$

where integration from actual vapor mass density concentration ρ_v to saturated concentration ρ_{vs} is used. It is also assumed that ρ_a remains constant, that is, for water $\rho_a = 1000$ kg/m^3.

The pressure p_{cap} can be assumed to be related to the mean curvature r_{cap} of the capillary condensed liquid through the material constant γ_a, which represents the surface tension of the adsorbate (or equally the surface energy). This relation is the Laplace equation, i.e.

$$p_{cap} = \gamma_a\left(\frac{1}{r_{cap}^1} + \frac{1}{r_{cap}^2}\right) = \frac{\gamma_a}{2r_{cap}} \tag{12}$$

where r_{cap}^1 and r_{cap}^2 are the radii of the curvature of the meniscus in two orthogonal directions. The property r_{cap} does not need to be equivalent to the pore radii in which the liquid is present if the so-called wetting angle α is different from zero. When allowing for different wetting angles between liquid and material the relation between the radii r_{cap} and the pore radii r_{pore} becomes

$$r_{cap} = \frac{r_{pore}}{\cos(\alpha)}. \tag{13}$$

From relations (11)–(13) the pore distribution can be estimated, i.e.

$$r_{pore} = -\frac{M_v 2\gamma_a\cos(\alpha)}{\rho_a R\theta\ln(x)} \tag{14}$$

which is the so-called Kelvin equation. It should be noted that when the relative humidity is low the water does not necessarily act as a capillary condensed liquid. Therefore the use of Eq. (14) should be restricted to medium and high relative humidities.

6. Results

The measured adsorption and desorption are presented for well-carbonated and noncarbonated cement mortar. The obtained specific surface areas for these two materials are calculated using the BET equation. The pore distribution is

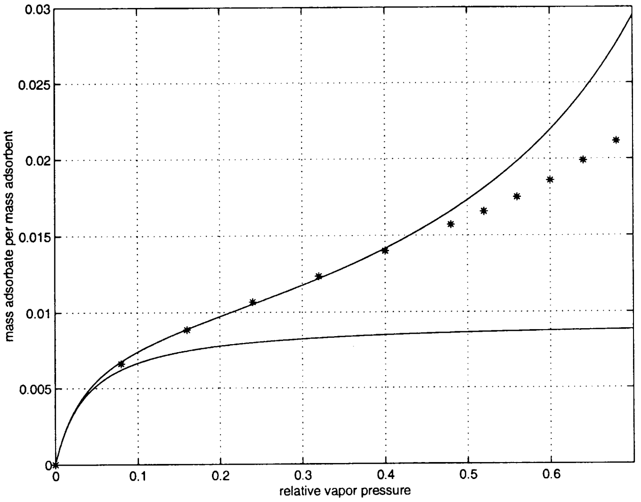

Fig. 2. Comparison between measured values (stars) and the BET equation (upper solid line) for noncarbonated cement mortar. The lower solid line represents the development of first layer adsorbate as predicted by the BET theory.

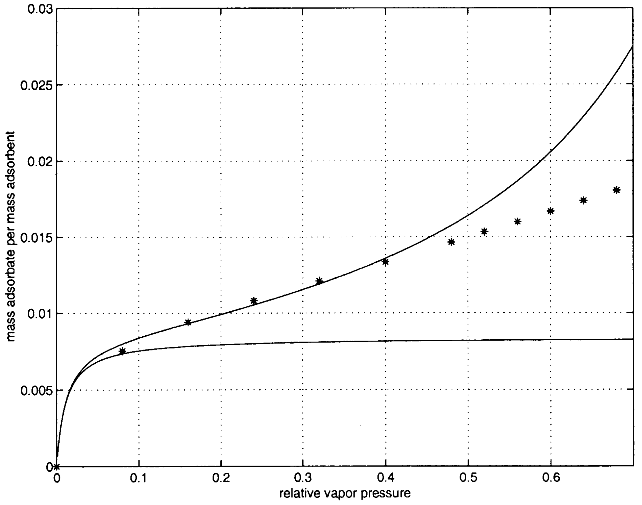

Fig. 3. Comparison between measured values (stars) and the BET equation (upper solid line) for well-carbonated cement mortar. The lower solid line represents the development of first layer adsorbate as predicted by the BET theory.

calculated from the measured desorption using the Kelvin equation [Eq. (14)].

In Figs. 2 and 3 the adsorption isotherms for non- and well-carbonated cement mortar are shown. Relative humidities up to 40% were used when fitting the measured values to the BET equation [Eq. (6)]. The best fitted BET equations are shown with solid lines in Figs. 2 and 3. A satisfying match for the whole range of 0–95% relative humidities tested could not be obtained as expected.

The noncarbonated cement mortar adsorbed more water at low relative humidities and less at high relative humidities than well-carbonated mortar.

The lower solid curve in Figs. 2 and 3 are the calculated development of volume adsorbent present in first layer, as a function of relative humidity. The relation $v_1 = v_m cx/(1-x+cx)$ is used, where v_1 is the mass adsorbate per mass adsorbent present in the first layer. This relation can be derived from the basic assumptions of the BET theory. By comparing the calculated development of the amount of molecules present in the first layer, for the two samples, as a function of relative humidity, it is concluded that v_1 reaches a constant value at a lower relative humidity for the well-carbonated cement mortar.

The material constants c and v_m corresponding to the fitted BET equations, shown in Figs. 2 and 3, are presented in Table 2. In this table the calculated specific surface areas S are also shown. The property S is assumed to be proportionally related to v_m, as described in Section 4. About 8% higher specific surface area was calculated for the noncarbonated mortar than for the well-carbonated sample. The most significant difference between the two different samples is the values of c, which differ by a factor about 3. This indicates that a higher differential condensation energy is required to place water molecules on bare material surfaces in well-carbonated cement paste than in noncarbonated mortar.

Table 2
Material constants and evaluation of specific surface area obtained from the BET equation

Material	c (−)	v_m (−)	S (m^2/g)
Noncarbonated	25.8	0.0090	31.8
Well-carbonated	89.8	0.0083	29.4

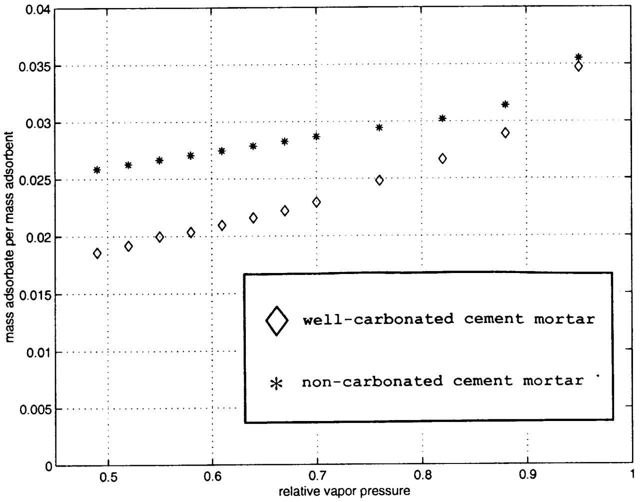

Fig. 4. Desorption (scanning) isotherms from 0.95 relative humidity obtained from equilibrium by adsorption.

In Fig. 4 the measured desorption isotherm for the two samples is shown. The measured points at 95% relative humidity were obtained by equilibration of predried samples through adsorption, i.e., the measured desorption shown represents scanning curves. According to the measurements presented in Fig. 4, the well-carbonated sample holds significantly less water at different relative humidities than

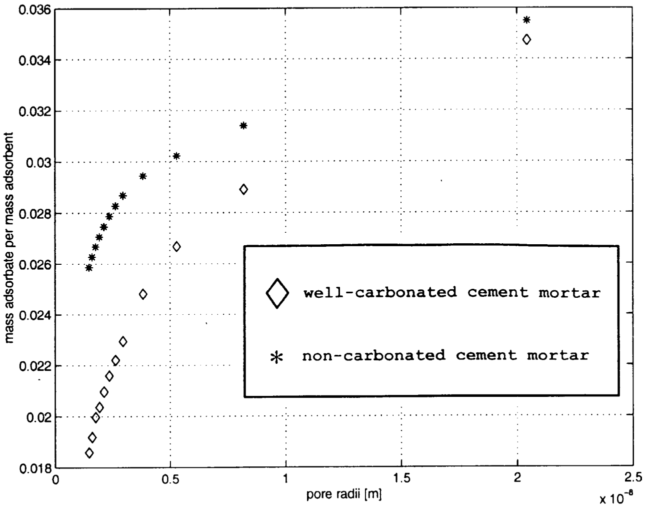

Fig. 5. Pore radii as a function of moisture content based on desorption measurements. The wetting angle was set to zero.

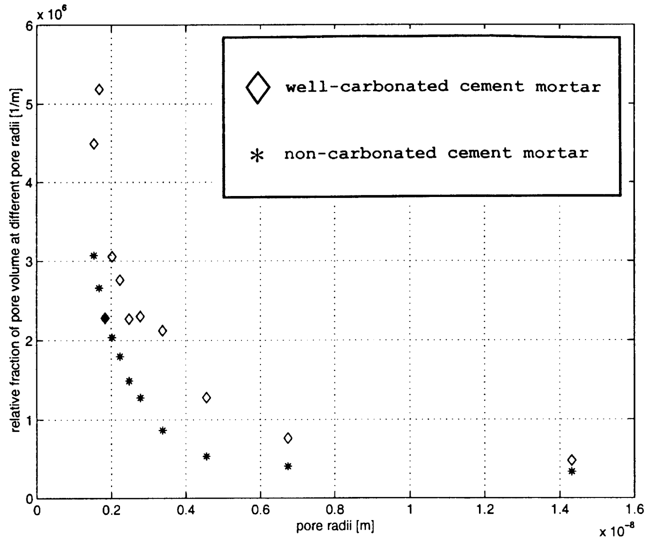

Fig. 6. Pore size distribution for well-carbonated and noncarbonated cement mortar. The values on the *y*-axis represent the slope of the curves presented in Fig. 5.

the noncarbonated cement mortar during desorption. This marked difference was not observed during adsorption in the range of humidities tested.

The *x*-axis in Fig. 4 has been rescaled to represent the pore radii, using Eq. (14). These plots are shown in Fig. 5 for the two tested materials. The wetting angle α was set to zero and the surface tension in use was $\gamma_a = 0.07197$ N/m, which is the value valid for liquid water at 25°C. The adsorption in the range 45% to 95% is neglected, thus all water in this range is assumed to be capillary condensed as described by the Kelvin equation.

The slopes of the curves presented in Fig. 5 are measures of the water present in different pore radii during desorption. These pore size distribution results are shown in Fig. 6. According to the assumptions described in Section 5, leading to the relation between the relative humidity and pore radii, and the results shown in Fig. 6, the well-carbonated cement mortar has a higher volume of cylindrical pores with radii in the range of 0.7×10^{-8}–0.2×10^{-8} m.

7. Discussion

A marked difference between the pore size distributions and a small difference in specific surface area was obtained for the noncarbonated and well-carbonated cement mortar used in this test. The results obtained should, however, be judged after the assumptions employed in the analysis. The simplest "one-layer" version of the BET equation was used according to which only the molecules adsorbed in first layer are assumed to have a condensation heat different from the normal heat of condensation. Assuming, for example, that second layers also have a special condensation heat, the calculated specific surface area will be different from the ones presented in Section 6. The obtained specific surface area is, further, dependent on the assumed range in which the BET theory is assumed to be valid. In this case 0–40% relative humidity was used. Making a best fit between measured adsorption and a BET equation in a smaller or larger range, the material constants c and v_m will be affected, hence the specific surface area will also be changed.

The pore size distributions as presented in Fig. 6 are based on the pores being capable of representation by perfectly shaped cylindrical pores in all size ranges. Furthermore, it is assumed that the wetting angle always is equal to zero. When the real conditions are significantly displaced from the assumed conditions the results should also be questioned. Another issue is at which range, in terms of relative humidities, the capillary condensation is active. In this work it was assumed that during adsorption from 95% to 50% only capillary condensation is active, and the molecular adsorption on surfaces is completely ignored.

8. Conclusions

It is concluded that carbonation only changes the specific surface area, as calculated by the BET equation, to a very small degree. The specific surface area obtained for the well-carbonated and noncarbonated cement mortar was 29.4 and 31.8 m^2/g, respectively. The differential energy required to adsorb water molecules at material surfaces is, however, according to the BET theory, much higher for well-carbonated cement mortar than for the noncarbonated sample.

If it is assumed that well-carbonated and noncarbonated cement mortar have the same wetting angle between capillary condensed water and pore walls, the calculated pore distributions using the Kelvin and Laplace relations reveal that the well-carbonated mortar has a significantly higher volume of pores in the pore size range of 0.7×10^{-8}–0.2×10^{-8} m. At adsorption the difference in the isotherms for the two tested samples was small. At desorption from 95% relative humidity (obtained by adsorption) the isotherm for the noncarbonated sample was significantly higher than for the well-carbonated sample, i.e., the noncarbonated cement mortar holds more water at desorption than the well-carbonated sample. The same conclusion has been reported in Ref. [6].

References

[1] P. Utgenannt, A Climate Chamber for Studies of the Effect of Carbonation, Swedish National Testing and Research Institute, Borås, 1999 (SP-report).

[2] K. Malmström, The Effect of Cement Type on the Frost Resistance of Concrete, Swedish National Testing and Research Institute, Borås, 1990 (SP-report, in Swedish).

[3] H.F.W. Taylor, Cement Chemistry, Academic Press, New York, 1990.

[4] D.W.S. Ho, R.K. Lewis, Carbonation of concrete and its predictions, Cem. Concr. Res. 17 (1987) 489–504.

[5] F.P. Glasser, E.E. Lachowski, D.E. Macphee, Compositional model for calcium silicate hydrate (C-S-H) gels: Their solubilities, and free energies of formation, J. Am. Ceram. Soc. 70 (7) (1987) 481–485.

[6] J. Kropp, Struktur und Eigenschaften Karbonatisierter Betonrandzonen, Bautenschutz Bausanierung 9 (1986) 33–39 (Jahrgang).